ELSEVIER

Journal of Hazardous Materials B136 (2006) 922–929

Journal of Hazardous Materials

www.elsevier.com/locate/jhazmat

Preparation of steam activated carbon from rubberwood sawdust (*Hevea brasiliensis*) and its adsorption kinetics

B.G. Prakash Kumar [a], K. Shivakamy [b], Lima Rose Miranda [a], M. Velan [a,*]

[a] *Department of Chemical Engineering, Alagappa College of Technology, Anna University, Chennai 600 025, India*
[b] *Centralised Waste Management Facility, Bhabha Atomic Research Centre, Kalpakkam 603 102, India*

Received 11 September 2005; received in revised form 6 December 2005; accepted 16 January 2006
Available online 28 February 2006

Abstract

Activated carbon was produced from a biowaste product, rubberwood sawdust (RWSD) using steam in a high temperature fluidized bed reactor. Experiments were carried out to investigate the influence of various process parameters such as activation time, activation temperature, particle size and fluidising velocity on the quality of the activated carbon. The activated carbon was characterized based on its iodine number, methylene blue number, Brauner Emmet Teller (BET) surface area and surface area obtained using the ethylene glycol mono ethyl ether (EGME) retention method. The best quality activated carbon was obtained at an activation time and temperature of 1 h and 750 °C for an average particle size of 0.46 mm. The adsorption kinetics shows that pseudo-second-order rate fitted the adsorption kinetics better than pseudo-first-order rate equation. The adsorption capacity of carbon produced from RWSD was found to be 1250 mg g^{-1} for the Bismark Brown dye. The rate constant and diffusion coefficient for intraparticle transport were determined for steam activated carbon. The characteristic of the prepared activated carbon was found comparable to the commercial activated carbon.

Keywords: Activated carbon; Steam activation; Fluidized bed reactor; Rubberwood sawdust; Adsorption

1. Introduction

Activated carbon is a unique and effective adsorbent for the separation and removal of unwanted organic matters from industrial effluents. It finds wide application in food, pharmaceuticals, solvent recovery, drinking water treatment, fuel cells [1], chemical and other process industries. Most of the activated carbons are produced by a two-stage process, carbonisation followed by activation. The first step is to enrich the carbon content and to create an initial porosity and the activation process helps in enhancing the pore structure. Considerable amount of work using fluidized bed reactor (FBR) for the preparation of activated carbon by steam/CO_2/N_2 from various sources has been carried out. Fossil materials like miike coal [2], Spanish HV bituminous coal char [3–5], semi anthracite char [6], coal and pitch coke [7], the shell-based agricultural wastes like coconut shell [8,9], palm shell [10,11], almond shell [12] and agricultural waste materials like olive seed waste residue [13,14], pine waste [15], pine wood [16] and wood char [17] have been used as a raw material. Steam activation at higher temperatures gave better activation and enhanced widening of the narrow micro-pore network. The steam gasification of oxicoke char [7] produced carbon with less micro-porous structure when compared to CO_2 gasification. This implies that the pore structure and adsorption properties of activated carbon are strongly influenced by physicochemical nature of precursor materials and the thermal history during the manufacturing process.

In the present work, a biowaste product rubberwood sawdust (RWSD) has been used as the precursor. Rubberwood (*Hevea brasiliensis*) is grown in the sunny slopes of South India (Kerala). In India, over 4.5 lakh Ha of land are under rubber cultivation, which is ranked third in the world. It is mainly grown for its latex and is cut down every 20 years. Beyond this age, these trees become unproductive and are necessarily felled as a part of the re-planting operations. Literature on production of activated carbon from RWSD by chemical activation [18–23] route is limited. Steam activated carbon (SAC) from RWSD has not

Abbreviations: RWSD, rubberwood sawdust; SAC, steam activated carbon; CAC, commercial activated carbon

* Corresponding author. Tel.: +91 44 22203506; fax: +91 44 22352642.
E-mail address: velan@annauniv.edu (M. Velan).

0304-3894/$ – see front matter © 2006 Elsevier B.V. All rights reserved.
doi:10.1016/j.jhazmat.2006.01.037

Nomenclature

a	radius of the adsorbent (m)
C_e	dye concentration at equilibrium (mg L^{-1})
C_0	initial dye concentration (mg L^{-1})
D_i	intraparticle diffusion coefficient (m^2 s^{-1})
k_p	rate constant of intraparticle transport (mg g^{-1} $min^{-1/2}$)
k_1	equilibrium rate constant of pseudo-first-order adsorption (min^{-1})
k_2	equilibrium rate constant of pseudo-second-order adsorption (g mg^{-1} min^{-1})
M	mass of the activated carbon (g)
Δq	standard deviation
q_e	adsorption capacity at equilibrium (mg g^{-1})
q_t	adsorption capacity at any time t (mg g^{-1})
V	volume of the dye solution (L)
W_f	final weight of product (g)
W_i	initial weight of the raw material (g)

been reported in the literature. Hence, RWSD is chosen for the preparation of activated carbon using steam.

The present work reports the influence of various process parameters such as activation time, activation temperature, particle size and fluidising velocity on the preparation of SAC using RWSD in a high temperature fluidized bed reactor (HTFBR).

Dyes are generally synthetic organic aromatic compounds, which is embodied with various functional groups. Removal of these dyes from industrial effluents is one of the vital environmental problems. Adsorption process has been accepted as one of the most appropriate processes, for the purification of water and wastewater. The adsorption of dyes on various adsorbents has been reported by many authors [24–28]. The adsorption kinetics as well as diffusion coefficient on steam activated carbon (SAC) of Bismark Brown (BB) dye was studied in the present work. The results are compared with a commercial activated carbon (CAC).

2. Materials and methods

2.1. Materials

Rubberwood sawdust as the precursor material was procured from Coimbatore (Tamilnadu, India). It was used to carry out the experiments and the proximate analysis of the raw material is shown in Table 1. Experiments were conducted in a HTFBR

Table 1
Proximate analysis of the rubberwood sawdust

Properties	Wet basis (wt.%)
Moisture	7.95
Fixed carbon	24.15
Volatile	62.91
Ash	4.95

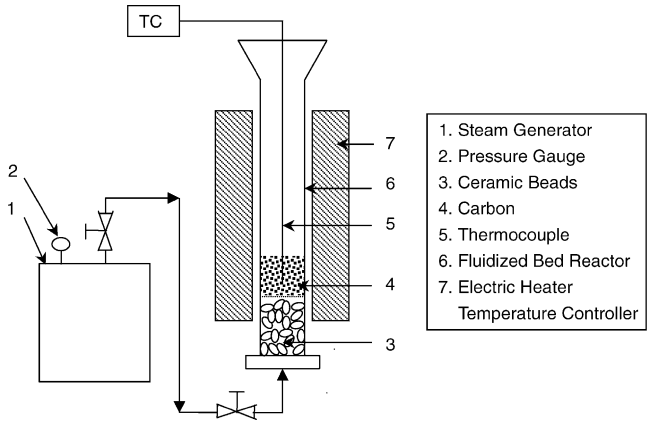

Fig. 1. Schematic diagram of high temperature fluidized bed reactor.

with 42 mm i.d. and 730 mm height operating between 600 and 800 °C and the schematic of the experimental set up is shown in Fig. 1. The flow rate of steam and the temperature in the reactor were controlled using suitable controllers.

2.2. Activation conditions

Sawdust of a particular particle size was thoroughly washed and dried. Ten grams of sample were used in each run. The process of converting sawdust to activated carbon was carried out in two stages: (1) carbonisation and (2) activation. Generally above 270–280 °C temperature, the wood substance begins to partially degrade with the evolution of carbon monoxide, carbon dioxide and acetic acid [29]. The source material was first carbonised at 400 °C in the self-generated atmosphere for residence time of 1 h. The burn-off percentage and iodine number of the carbonised char were found to be 60% and 262 mg g^{-1}, respectively. This indicates poor development of pore during the carbonisation stage. It was often found that the porosity of char was not always accessible due to pores being filled by disorganized carbon resulting from deposition of tar [29]. The carbonised char was then activated with steam in a HTFBR at different activation time (1–4 h) and temperature (600, 700 and 750 °C).

2.3. Characterization

The iodine (mg of iodine adsorbed/g of carbon) and methylene blue number (mg of methylene blue adsorbed/g of carbon) were determined according to ASTM 4607-86 and BIS 877-1977 standards, respectively. The burn-off weight percentage measures the degree of activation process. It is defined as the ratio of percentage weight decrease of the material during the preparation to the original weight of the raw material. It is mathematically expressed as

$$\text{percentage burn-off} = \frac{W_i - W_f}{W_i} \times 100 \quad (1)$$

where W_i is the initial weight of the raw material and W_f is the final weight of product. The surface area of the activated carbon was deduced from the adsorptions of N_2 at 77 K (Sorptomatic

1990, CE instrument) and also surface area by ethylene glycol mono ethyl ether (EGME) retention method [30–32].

2.4. Adsorption studies

A cationic dye Bismark Brown R (BB) (CI: 21010) was selected for the adsorption studies. The steam activated carbon from RWSD having the highest surface area was used for the batch adsorption studies. The equilibrium adsorption capacities (q_e) of the activated carbon at predetermined time intervals were determined based on adsorbate mass balance using Eq. (2):

$$q_e = \frac{(C_0 - C_e)V}{M} \quad (2)$$

where C_0 and C_e are the initial and equilibrium concentrations of the dye (mg L^{-1}), respectively, V the volume of the aqueous solution (L), and M is the mass of activated carbon used (g). The concentrations of the withdrawn samples were measured using UV–vis spectrophotometer (Hitachi U 2000) at 470 nm for BB dye. The kinetic parameters for the adsorption process were determined and compared with commercial activated carbon (CAC) (E-Merck brand).

3. Results and discussion

3.1. Influence of various process parameters on preparation of activated carbon

3.1.1. Effect of activation temperature

When the activating agent comes in contact with the char, it reacts both with the exterior and the interior of the particle, in which most of the disorganized carbon is removed. With regard to the effect of activation temperature, the results indicate burn-off range of 75–88% (Table 2). The BET surface area increased gradually with activation temperature (600–750 °C) and a rapid increase of surface area was observed for particle size of 0.46 mm at 750 °C (Table 2). This is due to the fact that, at higher temperature, the diffusion rate of the water molecules to the interior is higher for the smaller particle size, which develops a wide range of pore network. When the activation temperature increased above 750 °C, it was found that the particles were burnt out completely. The highest iodine and methylene blue number of 765 and 255 mg g^{-1} was obtained for the 0.46 mm particle size, which indicates development of mesopores. For the steam activation process, development of mesoporosity to a higher extent was reported in the literatures [3–6,14,17].

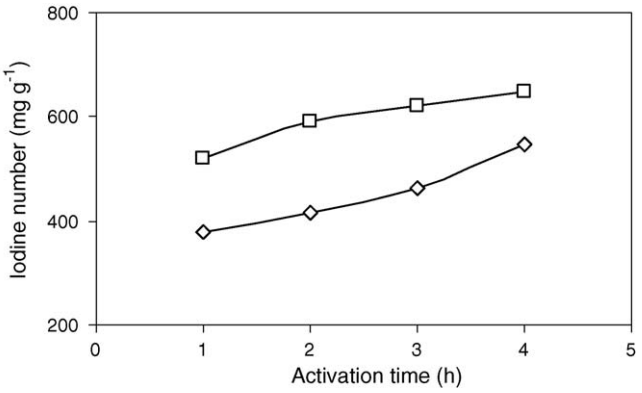

Fig. 2. Effect of activation time on iodine number for 600 and 700 °C activation temperatures ((◊) 600 °C; (□) 700 °C).

3.1.2. Effect of activation time

The effect of activation time on iodine number for various temperatures and particle size of 0.46 mm are shown in Figs. 2 and 3. Increase in activation time up to 4 h showed that the iodine number increased slowly when the activation temperature was 600 and 700 °C. At 750 °C the activation time was varied from 10 to 60 min and rapid increase of iodine was observed with a maximum value of 765 mg g^{-1}. Further increase in activation time at 750 °C leads to complete burn off due to very high gasification rates. The observed trend agreed with those reported in the literatures [8,13].

3.1.3. Effect of fluidising velocity ratio (U/U_{mf})

The effect of U/U_{mf} ratio (1.0–1.8) on iodine number for various particle sizes is shown in Fig. 4. It was found that there was no substantial variation, which means change in porosity variation was negligible. At higher ratio, complete burnout of the carbon char was observed at higher activation temperature.

Table 2
Properties of steam activated carbon

Particle size (mm)	Temperature (°C)	Iodine number (mg g^{-1})	Methylene blue number (mg g^{-1})	S_{BET} (m^2 g^{-1})	S_{EGME} (m^2 g^{-1})	Burn-off (%)
0.46	600	358	15	353	334	78
	700	521	53	529	488	81
	750	765	255	1092	867	88
0.93	600	320	15	305	310	78
	700	488	45	497	450	79
	750	702	143	500	752	85
1.31	600	300	0	279	298	75
	700	411	30	415	375	76
	750	677	83	495	710	84
CAC	–	850	210	1095	1250	–

CAC: commercial activated carbon.

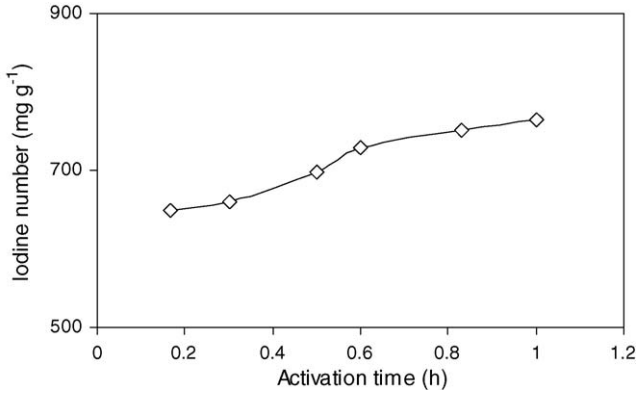

Fig. 3. Effect of activation time on iodine number for 750 °C activation temperatures.

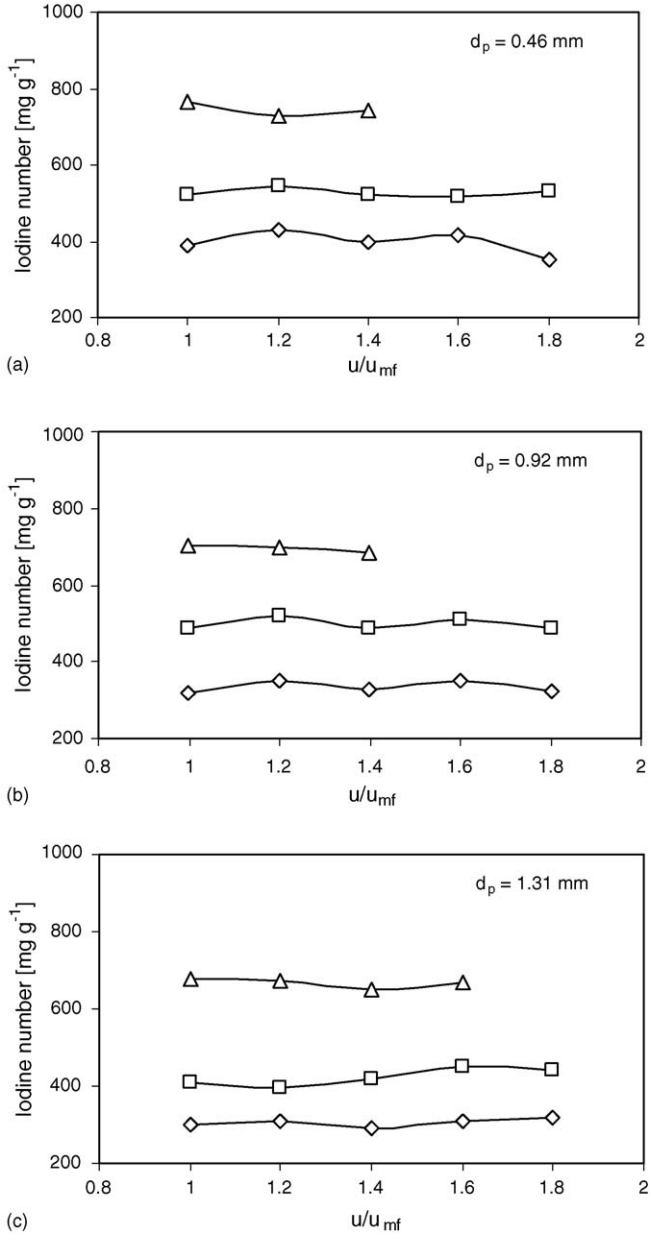

Fig. 4. Effect of U/U_{mf} ratio on iodine number for various particle sizes and different activation temperatures with activation time of 1 h ((◊) 600 °C; (□) 700 °C; (△) 750 °C).

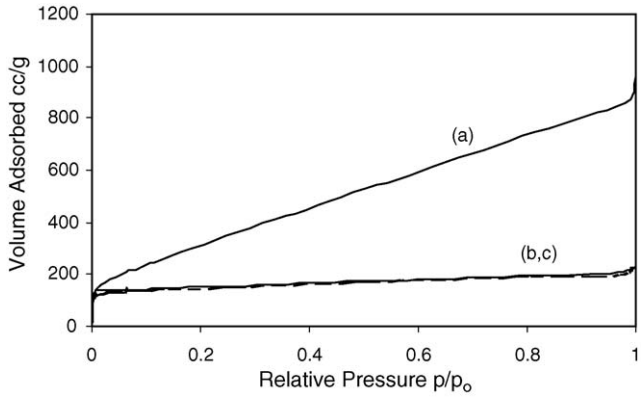

Fig. 5. N_2 adsorption isotherms for various particle size carbons, activated at 750 °C: (a) 0.46; (b) 0.93; (c) 1.31 mm.

Negligible effect of fluidising velocity ratio on the iodine number for the activation of 0.55 mm coconut shell particles in a FBR using CO_2 as a fluidising medium was reported by Satya Sai et al. [8]. John et al. [33] observed that changes in fluidising velocity slightly affected the carbon consumption rate at higher temperature (>1000 °C) for small particles (d_p = 188 μm) in the metallurgical coke gasification using CO_2/N_2 mixture in FBR.

3.1.4. Effect of particle size

With increase in particle size the iodine and methylene blue number, surface area and burn-off percentage showed a decreasing trend (Table 2). The highest burn-off percentage was observed for the 0.46 mm particles at the highest temperature, which indicates the removal of more of the tarry materials from the carbon. Higher values of iodine, methylene blue number and surface area were obtained for the 0.46 mm particles. Similar trend was reported by Hashimoto et al. [2] and Al-Khalid et al. [13] for the activation miike coal and olive seed waste residue in a FBR using steam and CO_2 as the activating agents, respectively.

The N_2 adsorption isotherms for different sizes of activated carbon prepared at 750 °C is shown in Fig. 5. It was found that there was significant difference in the knee and slope of the linear portion for 0.46 mm (Type I isotherm) and other two particles (0.93 and 1.31 mm) (Type II isotherm) [34]. The observance of sharp knee and horizontal isotherm for 0.93 and 1.31 mm activated carbon particles indicates the occurrence of narrow microporosity. In the case of 0.46 mm particles, open knee at low relative pressure and steeper slope at higher relative pressure represents transition from microporosity to mesoporosity. A large positive difference between N_2 BET surface area (S_{BET}) and EGME surface area (S_{EGME}) was observed for 0.46 mm particles at 750 °C while minimum deviation was observed for the other size ranges. Similar trend was reported by Molina-Sabio et al. [31]. Thus, for smaller particle, well-developed micropore as well mesopores were obtained when compared to larger particle size.

3.2. SEM studies

The surface morphologies of the activated carbon produced was determined using scanning electron microscopy (JSM-

840A Scanning Microscope, Jeol-Japan). Fig. 6(a) and (b) shows the SEM photographs of the RWSD at 750 °C for particle size of 0.46 mm at 1000× and 2000× magnifications, respectively. It was observed that the activated carbon has smooth surface areas with long ridges, resembling a series of parallel lines. The straight tubes each with nearly uniform dimensions are evident in these figures. Based on the outward appearance it can be said that the pores are not cross-linked. Hard woody material gives cross-interconnected pores while softer woody material gives fibrillar structure in nature [35].

3.3. Adsorption of BB dye

3.3.1. Adsorption kinetics

For the adsorption kinetics the highest surface area RWSD steam activated carbon (SAC) was used and compared with commercial activated carbon (CAC) The kinetics of adsorption was analyzed using Legergren's pseudo-first-order and pseudo-second-order rate equations [25]. A simple kinetic analysis of adsorption is the Legergren's pseudo-first-order differential equation is

$$\frac{dq}{dt} = k_1(q_e - q) \tag{3}$$

Integrating Eq. (3) for the boundary conditions $t = 0$ to t and $q = 0$ to q, gives:

$$\log(q_e - q) = \log q_e - \frac{k_1 t}{2.303} \tag{4}$$

where q and q_e is the amount of dye adsorption at any time t (min) and equilibrium (mg g^{-1}), k_1 is the equilibrium rate constant of first-order adsorption (min^{-1}).

For the rate constant of the pseudo-second-order adsorption process the differential equation is

$$\frac{dq}{dt} = k_2(q_e - q)^2 \tag{5}$$

Integrating Eq. (5) for the boundary conditions $t = 0$ to t and $q = 0$ to q, gives:

$$\frac{t}{q} = \frac{1}{k_2 q_e^2} + \frac{t}{q_e} \tag{6}$$

where q and q_e is the amount of dye sorbed at time t and at equilibrium (mg g^{-1}), k_2 is the equilibrium rate constant of second-order adsorption (g mg^{-1} min^{-1}).

In order to quantitatively compare the applicability of models studied, a normalized standard deviation Δq is calculated from

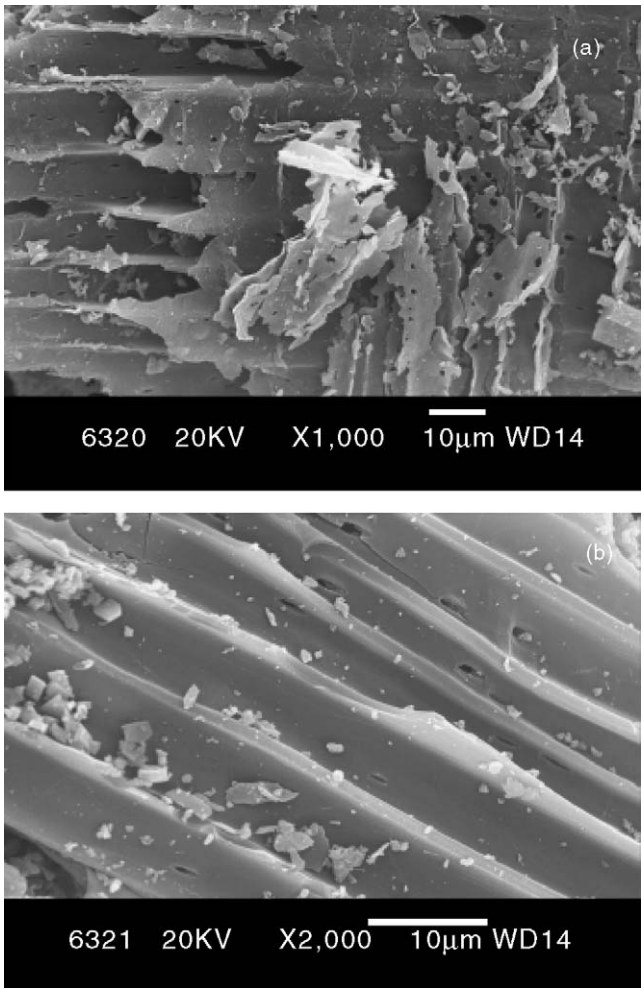

Fig. 6. (a) and (b) SEM micrographs of RWSD.

Eq. (7):

$$\Delta q\,(\%) = 100 \times \sqrt{\frac{\sum [(q_{t,\mathrm{exp}} - q_{t,\mathrm{cal}})/q_{t,\mathrm{exp}}]^2}{n-1}} \tag{7}$$

where n is the number of data points. The adsorption rate constants for BB dye calculated from plots (figures not shown) are presented in Table 3. The results show that the pseudo-second-order rate equation agrees well with experimental data for both the carbons (Figs. 7 and 8), the linear regression co-efficient of 0.99 and standard deviation % are less (Table 3) when compared to the pseudo-first-order rate equation. The uptake capacity of SAC and CAC for BB dye was found to be 1250 and 250 mg g^{-1}, respectively. Hence, it was found that the carbon produced from RWSD have higher adsorption capacity than the commercial activated carbon.

Table 3
Adsorption kinetic model constants for the Bismark Brown dye for both the carbons

Adsorbent	Pseudo-first order			Pseudo-second order				Intraparticle diffusion		
	k_1 (min^{-1})	R^2	Δq (%)	k_2 (g mg^{-1} min^{-1})(×10^3)	q_e (cal) (mg g^{-1})	R^2	Δq (%)	k_p (mg g^{-1} min$^{-1/2}$)	R^2	Δq (%)
SAC	0.185	0.96	43.34	8.0	1250	0.99	25.58	124.34	0.95	7.58
CAC	0.061	0.80	54.34	1.4	250	0.99	7.18	25.87	0.97	3.32

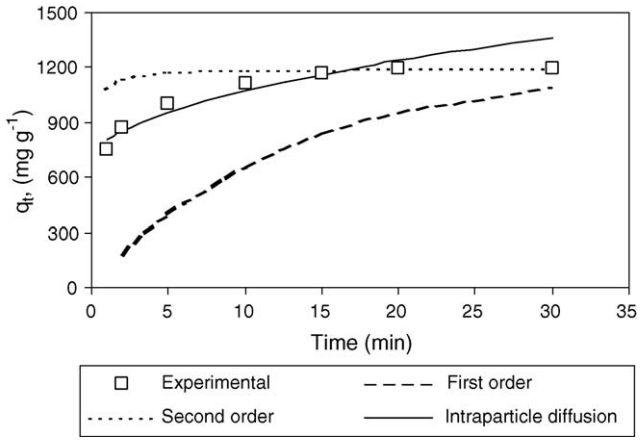

Fig. 7. Typical plot of comparison between the experimental and modeled time profiles for adsorption of BB dye on SAC.

The results showed that the performance of carbon produced in the present study was much better when compared to the results reported by Choa et al. [36] and Bhatnagar and Jain [37] for the adsorption of Bismark Brown Y on to chitosan (48.8 mg g^{-1}) and Bismark Brown R on to blast furnace sludge (85 mg g^{-1}), respectively. Hence, activated carbon from RWSD can be employed as low cost adsorbent and considered as an alternative to CAC.

3.3.2. Diffusion coefficient

The intraparticle diffusion model presented here refers to the theory proposed by Weber and Morris [38] who concluded that the uptake is proportional to the square root of contact time during the course of adsorption. Accordingly:

$$q_t = k_p \sqrt{t} \tag{8}$$

where k_p (mg g^{-1} $min^{-1/2}$) is the rate constant of intraparticle transport. The intraparticle diffusion plot may present a mutilinearity, indicating that two or more steps take place [39]. The general features of the plot are initial curved portion followed by linear portion and a plateau. The slope of the linear portion has

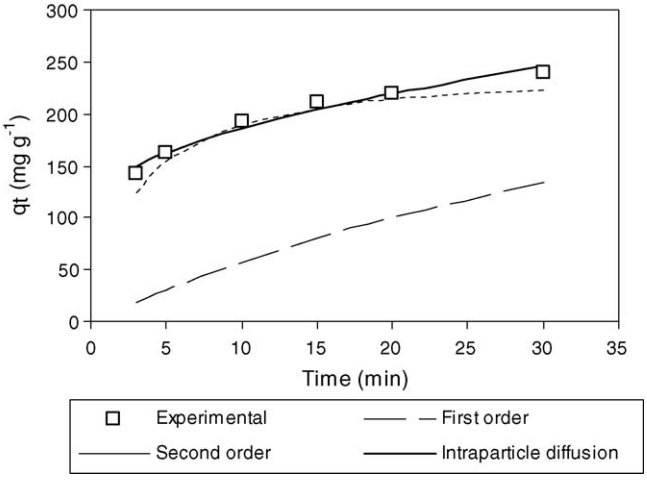

Fig. 8. Typical plot of comparison between the experimental and modeled time profiles for adsorption of BB dye on CAC.

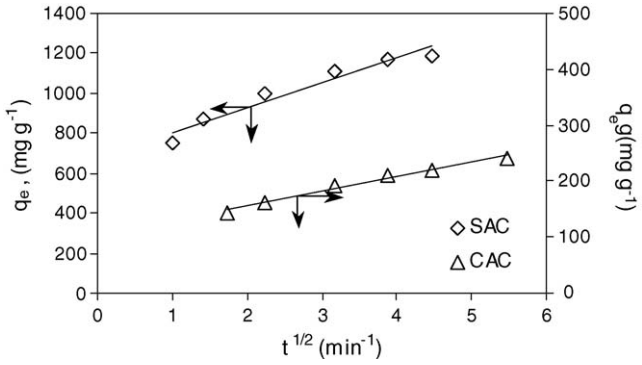

Fig. 9. Plot of intraparticle diffusion model for the adsorption of BB dye on SAC and CAC carbons.

been defined as a rate parameter (k_p) and characteristic of the rate of adsorption in this region where intraparticle diffusion is rate limiting and were obtained as 124.34 and 25.87 mg g^{-1} $min^{-1/2}$ for SAC and CAC, respectively. From Fig. 9, it may be observed that the straight line did not pass through the origin and this further indicates that the intraparticle diffusion is not only the rate controlling step. That adsorption data indicate that the removal of BB dye from aqueous solution is rather complex process involving both boundary layer diffusion and intraparticle diffusion. This phenomena has been reported by the adsorption of malachite green on *Prosopis cineraria* [28].

To evaluate the intraparticle diffusion coefficient (D_i), assuming adsorbent particle to be sphere of radius 'a' and the diffusion follows Fick's law. The relationship between weight uptake and time is given by Crank [40]:

$$\frac{q_t}{q_e} = 1 - \frac{6}{\pi^2}\sum_{n=1}^{\infty}\frac{1}{n^2}\exp\left(-\frac{Dn^2\pi^2 t}{a^2}\right) \tag{9}$$

As t tends to long time, the D represents D_i and Eq. (10) can be written in the form:

$$\ln\left(1 - \frac{q_t}{q_e}\right) = \ln\frac{6}{\pi^2} - \left(\frac{D_i\pi^2}{a^2}t\right) \tag{10}$$

D_i calculated from the slope of the plot of $\ln(1 - q_t/q_e)$ versus t as shown in Fig. 10. The values of D_i are found to be 2.312×10^{-12} and 1.12×10^{-12} m^2 s^{-1} for SAC and CAC, respectively. If intraparticle or pore diffusion is to be the rate

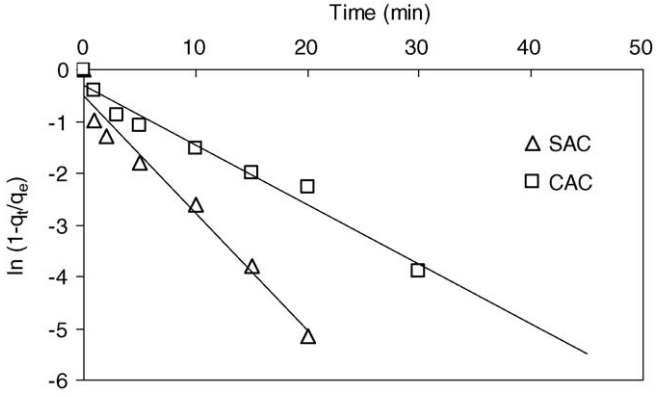

Fig. 10. Plot of intraparticle diffusion coefficient model for SAC and CAC carbons.

limiting step the diffusion coefficient should be in the range of 10^{-12} to 10^{-14} $m^2 s^{-1}$ [41]. Here the values of D_i are in the order of 10^{-12} $m^2 s^{-1}$, indicating the results are consistent with the other reported results [42,43].

4. Conclusions

The best conditions for the preparation of activated carbon from RWSD using steam activation was found at activation temperature of 750 °C and an activation time of 1 h for 0.46 mm particle size. The iodine number, BET surface area and EGME surface area of carbon produced under best conditions are 765, 1092 and 867 $m^2 g^{-1}$, respectively. The pseudo-second-order rate equation fitted the experimental data better when compared to the pseudo-first order. The maximum adsorption capacity of carbon produced from RWSD was found to be 1250 mg g^{-1} for the Bismark Brown dye adsorption. The adsorption study shows that RWSD activated carbon appears to be an interesting natural material for the production of activated carbon.

References

[1] J. Maruyama, I. Abe, Enhancement effect of an adsorbed organic acid on oxygen reduction at various types of activated carbon loaded with platinum, J. Power Sources 148 (2005) 1–8.
[2] K. Hashimoto, K. Miura, F. Yoshikawa, I. Imai, Change in pore structure of carbonaceous materials during activation and adsorption performance of activated carbon, Ind. Eng. Chem. Process. Des. Dev. 18 (1979) 72–79.
[3] A. Linares-Solano, I. Martín–Gullón, L.C. Salinas-Martínez, B. Serrano-Talavera, Activated carbons from bituminous coal: effect of mineral matter content, Fuel 79 (2000) 635–643.
[4] A. Linares-Solano, Salinas-Martínez de Lecea, D. Cazorla-Amorós, I. Martín-Gullón, Porosity development during CO_2 and steam activation in a fluidized bed reactor, Ener. Fuels 14 (2000) 142–149.
[5] I. Martín-Gullón, M. Asensio, R. Font, A. Marcilla, Steam activated carbons from a bituminous coal in a continuous multistage fluidized bed pilot plant, Carbon 34 (1996) 1515–1520.
[6] J.B. Parra, J.C. Sousa, J.J. Pis, J.A. Pajares, R.C. Bansal, Effect of gasification on the porous characteristics of activated carbons from a semi anthracite, Carbon 33 (1995) 801–807.
[7] H. Kühl, M.M. Kashani-Motlagh, H.J. Mühlen, K.H. Van Heek, Controlled gasification of different carbon material and development of pore structure, Fuel 71 (1992) 879–882.
[8] P.M. Satya Sai, J. Ahmed, K. Krishnaiah, Production of activated carbon from coconut shell char in a fluidized bed reactor, Ind. Eng. Chem. Res. 36 (1997) 3625–3630.
[9] W.M.A.W. Daud, W.S.W. Ali, Comparison on pore development of activated carbon produced from palm shell and coconut shell, Bioresour. Technol. 93 (2004) 63–69.
[10] W.M.A.W. Daud, W.S.W. Ali, M.Z. Sulaiman, Effect of activation temperature on pore development in activated carbon produced from palm shell, J. Chem. Technol. Biotechnol. 78 (2003) 1–5.
[11] J.S. Tan, F.N. Ani, Diffusional behavior and adsorption capacity of palm shell chars for oxygen and nitrogen—effect of carbonization temperature, Carbon 41 (2003) 840–842.
[12] C.A. Toles, W.E. Marshall, L.H. Wartelle, A. McAloon, Steam or carbon dioxide activated carbons from almond shells: physical, chemical and adsorptive properties and estimated cost of production, Bioresour. Technol. 75 (2000) 197–203.
[13] T.T. Al-Khalid, N.M. Haimour, S.A. Sayed, B.A. Akash, Activation of olive-seed waste residue using CO_2 in a fluidized-bed reactor, Fuel Process. Technol. 57 (1998) 55–64.
[14] F. Rodríguez-Reinoso, M. Molina-Sabio, M.T. González, The use of steam and CO_2 as activating agents in the preparation of activated, Carbon 33 (1995) 15–23.
[15] A. García-García, A. Gregório, C. Franco, F. Pinto, D. Boavida, I. Gulyurtlu, Unconverted chars obtained during biomass gasification on a pilot-scale gasifier as a source of activated carbon production, Bioresour. Technol. 88 (2003) 27–32.
[16] R.L. Tseng, F.C. Wu, R.S. Juang, Liquid-phase adsorption of dyes and phenols using pinewood-based activated carbons, Carbon 41 (2003) 487–495.
[17] M.F. Tennant, D.W. Mazyck, Steam pyrolysis activation of wood char for superior odorant removal, Carbon 41 (2003) 2195–2202.
[18] P. Chuenklang, S. Thungtong, T. Vitidsant, Effect of activation by alkaline solution on properties of activated carbon from rubber wood, J. Metal Mater. Mineral 12 (2002) 29–38.
[19] C. Raji, G.N. Manju, T.S. Anirudhan, Removal of heavy metal ions from water using sawdust-based activated carbon, Ind. J. Eng. Mater. Sci. 4 (1997) 254–260.
[20] C. Raji, T.S. Anirudhan, Copper-impregnated sawdust carbon for the treatment of As(III) rich water, J. Scientific Ind. Res. 57 (1998) 10–15.
[21] S. Hasan, M.A. Hashim, B.S. Gupta, Adsorption of $Ni(SO_4)$ on Malaysian rubber-wood ash, Bioresour. Technol. 72 (2000) 153–158.
[22] W. Somboon, P. Mutitamongkol, P. Tanpaiboonkul, Removal of colored wastewater generated from hand-made textile weaving industry, in: Fourth Asia Pacific Roundtable for Cleaner Production, Regional Conference, Thailand, 2003.
[23] C. Srinivasakannan, M.Z. Abu Bakar, Production of activated carbon from rubber wood sawdust, Biomass Bioener. 27 (2004) 89–96.
[24] C. Namasivayam, K. Kadirvelu, Activated carbons prepared from coir pith by physical and chemical activation methods, Bioresour. Technol. 62 (1997) 123–127.
[25] Y.S. Ho, G. McKay, Sorption of dye from aqueous solution by peat, Chem. Eng. J. 70 (1998) 115–124.
[26] F.C. Wu, R.L. Tseng, R.S. Juang, Pore structure and adsorption performance of the activated carbons prepared from plum kernels, J. Hazard. Mater. B69 (1998) 287–302.
[27] M.F.R. Pereira, S.F. Soares, J.J.M. Órfão, Adsorption of dyes on activated carbons: influence of surface chemical groups, Carbon 41 (2003) 811–821.
[28] V.K. Garg, R. Kumar, G. Renuka, Removal of malachite green dye from aqueous solution by adsorption using agro-industry waste: a case study of *Prosopis cineraria*, Dyes Pigments 62 (2004) 1–10.
[29] M. Smisek, S. Cerny, Active Carbon: Manufacture, Properties and Application, Elsevier Amsterdam/New York 1970.
[30] B.R. Puri, D.D. Singh, U. Gupta, Ethylene glycol retention method for estimating specific surface area of adsorbent carbons, Carbon 17 (1979) 121–123.
[31] M. Molina-Sabio, Salinas-Martínez de Lecea, F. Rodríguez-Reinoso, C. Puente-Ruiz, A. Linares Solano, A comparison of different tests to evaluate the apparent surface area of activated carbons, Carbon 23 (1985) 91–96.
[32] A.B. Cerato, A.J. Lutenegger, Determination of surface area of fine-grained soils by the ethylene glycol monoethyl ether (EGME) method, Geotech. Testing J. 25 (2002) 1–9.
[33] F.S. John, D. Barrett, H.T. Duong, Fluidised bed gasification of a metallurgical coke with CO_2/N_2 mixture, Can. J. Chem. Eng. 63 (1985) 936–944.
[34] S.J. Allen, L. Whitten, G. McKay, The production and characterisation of activated carbons: a review, Dev. Chem. Eng. Mineral Process 6 (1998) 231–261.
[35] R. Malik, M. Mukherjee, A. Swami, D.S. Ramteke, S. Rajkamal, Validation of adsorption efficiency of activated carbons through surface morphological characterization using scanning electron microscopy technique, Carbon Sci. 5 (2004) 75–80.
[36] A.C. Choa, S.S. Shyu, Y.C. Lin, F.L. Mi, Enzymatic grafting of carboxyl groups on to chitosan-to confer on chitosan the property of a cationic dye adsorbent, Bioresour. Technol. 91 (2004) 157–162.

[37] A. Bhatnagar, A.K. Jain, A comparative adsorption study with different industrial wastes as adsorbents for the removal of cationic dyes from water, J. Coll. Interf. Sci. 281 (2005) 49–55.
[38] W.J. Weber, J.C. Morris, Kinetics of adsorption on carbon solution, J. San. Eng. Div. ASCE 89 (1963) 31–59.
[39] G. McKay, Adsorption of dyestuffs from aqueous solution using activated carbon. III. Intraparticle diffusion processes, J. Chem. Technol. Biotechnol. 33A (1983) 196–204.
[40] J. Crank, The Mathematics of Diffusion, 2nd ed., Clarendon Press, Oxford, 1975.
[41] M. Streat, J.W. Patrick, M.J. Camporro Perez, Sorption of phenol and para-chlorophenol from water using conventional and novel activated carbon, Water Res. 29 (1995) 467–472.
[42] V.P. Vinod, T.S. Anirudhan, Effect of experimental variables on phenol adsorption on activated carbon prepared from coconut husk by single-step steam pyrolysis: mass transfer process and equilibrium studies, J. Scientific Ind. Res. 61 (2002) 128–138.
[43] F.C. Wu, R.L. Tseng, R.S. Juang, Kinetic modelling of liquid-phase adsorption of reactive dyes and metal ions on chitosan, Water Res. 35 (2001) 613–618.